PHYSICAL REVIEW B **93**, 020507(R) (2016)

Interface-enhanced electron-phonon coupling and high-temperature superconductivity in potassium-coated ultrathin FeSe films on $SrTiO_3$

Chenjia Tang,[1] Chong Liu,[1] Guanyu Zhou,[1] Fangsen Li,[1] Hao Ding,[1] Zhi Li,[1] Ding Zhang,[1] Zheng Li,[1] Canli Song,[1,2] Shuaihua Ji,[1,2] Ke He,[1,2] Lili Wang,[1,2,*] Xucun Ma,[1,2] and Qi-Kun Xue[1,2,†]

[1]*State Key Laboratory of Low-Dimensional Quantum Physics, Department of Physics, Tsinghua University, Beijing 100084, People's Republic of China*

[2]*Collaborative Innovation Center of Quantum Matter, Beijing 100084, People's Republic of China*

(Received 26 August 2015; revised manuscript received 13 January 2016; published 26 January 2016)

Alkali-metal (potassium) adsorption on FeSe thin films with thickness from 2 unit cells (UC) to 4 UC on $SrTiO_3$ grown by molecular beam epitaxy is investigated with a low-temperature scanning tunneling microscope. At appropriate potassium coverage (0.20–0.25 monolayer), the tunneling spectra of the films all exhibit a superconductinglike gap which is overall larger than 11 meV (five times the gap value of bulk FeSe) and decreases with increasing thickness, and two distinct features of characteristic phonon modes at ∼11 and ∼21 meV. The results reveal the critical role of the interface-enhanced electron-phonon coupling for possible high-temperature superconductivity in ultrathin FeSe films on $SrTiO_3$ and is consistent with recent theories. Our study provides compelling evidence for the conventional pairing mechanism for this type of heterostructure superconducting system.

DOI: 10.1103/PhysRevB.93.020507

A recent report on the high-T_C superconductivity in the heterostructure of single unit-cell (UC) FeSe films on $SrTiO_3$ (STO) (001) substrates grown by molecular beam epitaxy (MBE) [1] has stimulated considerable research interests in the superconductivity community. The FeSe/STO system displays superconducting gaps $\Delta\sim$15–20 meV [2–6] and T_C above 65 K [7–10], almost one order of magnitude higher than the values ($\Delta\sim$2.2 meV and $T_C \sim 8$ K) of bulk FeSe [11,12]. Interestingly, a unique Fermi surface topology is found in FeSe/STO: only electronlike pockets exist at the Brillouin zone corners and no hole pockets in the Brillouin zone center [2–5], which has experimentally been demonstrated to be induced by charge transfer from the oxygen vacancies in the STO substrates to 1-UC FeSe films above [2–5,13]. On the other hand, with hole pockets appearing in the Brillouin zone center and becoming stronger with increasing thickness [2,4,5], multilayer (≥2-UC) films on STO prepared by the same method do not exhibit any signature of superconductivity [1,2,4–6].

Considering the fact that the superconductivity in cuprate and iron-based layered superconductors is similarly achieved by doping (of a parent Mott insulator or metallic compound) and that the transition temperature T_C could be tuned by the amount of doped carriers in a phase diagram [14,15], one may speculate that the absence of superconductivity in multilayer FeSe films is due to insufficient carrier transfer from the STO substrate. This is demonstrated by a recent temperature-dependent angle-resolved photoemission spectroscopy (ARPES) study which shows that, once coated with potassium (K) atoms, 3-UC FeSe films become electron populous and exhibit a pairing formation temperature of 48 ± 3 K at optimal doping [16]. By observing a dome-shaped phase diagram, the study suggests that the high T_C probably comes from antiferromagnetic fluctuation that is enhanced at the interface and facilitated by forming some ordered phase. However, there is no proof for the parent ordered phase, thereby its link to the antiferromagnetic interaction enhancement or suppression as a function of doping level is speculative.

Similar to our initial proposal [1], the coupling between electrons and phonons that drives the formation of electron pairs as in conventional superconductors has been suggested to be responsible for the high T_C in FeSe/STO, which is evidenced by the ARPES observation of shake-off bands [5]. This observation suggests the important role of electron-phonon coupling. In conventional superconductors, the electron-phonon (e-ph) coupling is characterized by the dips in the second derivative of tunneling conductance (d^2I/dV^2) that correspond to the peaks in the Eliashberg spectral function $\alpha^2F(\omega)$ at energy $E = \Omega + \Delta$ (Ω is the phonon energy and Δ the superconducting gap) [17–21]. Such features were observed in high-temperature superconductors and often interpreted as bosonic modes [22–25]. However, the nature of those bosons and hence the pairing mechanism is under hot debate.

In this work, by measuring tunneling conductance (dI/dV) of bare 1-UC and K-coated 2-4-UC FeSe thin films on STO with the scanning tunneling microscopy/spectroscopy (STM/STS) technique, we find that 2–4-UC FeSe films become superconducting at appropriate K coverage and exhibit a U-shaped gap which is overall larger than 11 meV and decreases with increasing thickness. Furthermore, similar to conventional superconductors, the emergence of the superconducting gap is always accompanied with characteristic phonon modes, whose frequencies are ∼11 and ∼21 meV for all of the K-coated 2-4-UC FeSe films and bare 1-UC FeSe films. Our experimental finding further demonstrates the pivotal role of charge transfer and e-ph coupling in this system and thus supports our initial proposal of the interface enhancement reported in Ref. [1].

*liliwang@mail.tsinghua.edu.cn
†qkxue@mail.tsinghua.edu.cn

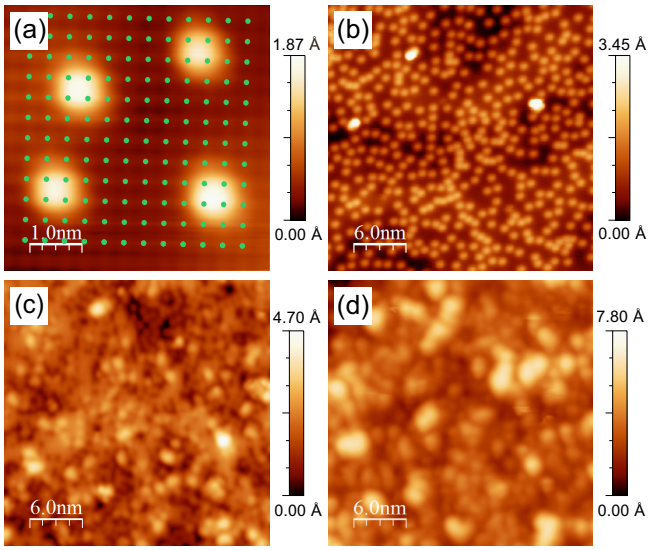

FIG. 1. Topographic images of the surface with K adsorption at various coverages. (a) 0.06 ML ($V = 500$ mV, $I = 50$ pA), (b) 0.08 ML, (c) 0.20 ML, and (d) 0.30 ML ($V = 1V$, $I = 30$ pA). The green dots in (a) show the positions of Se atoms.

The FeSe thin films were grown on STO substrates by MBE; the details of the growth can be found in our previous studies [1,7]. To directly compare the properties of adjacent layers on the same sample, we have prepared FeSe films with nominal thickness of $(n + 1/2)$ UC to obtain n-UC and $(n + 1)$-UC films simultaneously [26]. Potassium (K) atoms with coverage from 0.01 monolayer (ML) to 0.30 ML were successively deposited onto the FeSe films cooled down below 100 K by liquid nitrogen. Here, 1 ML is defined as the coverage at which K atoms occupy all the hollow sites of the Se lattice as in the case of stoichiometric $K_1Fe_2Se_2$ [27]. After K deposition, the samples were immediately transferred to the STM stage cooled at 4.6 K for STM measurements [28]. In all STM/STS measurements, a polycrystalline PtIr tip was used. The STS was acquired by using a lock-in technique with a bias modulation of 0.5 mV at 437 Hz.

Figure 1 shows the topographic STM images of K-coated FeSe films. Below 0.20 ML, K atoms adsorb individually on the surface and occupy the hollow sites of the (1×1) Se terminated (001) surface. With increasing coverage, some of the K atoms pile up and form clusters. Regardless of the cluster formations, we see no change in the overall film terrace-step morphology even at the maximum coverage, 0.30 ML. Thus, we assume that the structure of underlying FeSe films remains undisturbed, and the major change is in the electron density owing to electron donation from K adatoms (probably also from clusters), which converts the films into a superconducting state as discussed below.

Figure 2 summarizes the differential tunneling spectra (dI/dV) of 2-4-UC films taken at various K coverages. We can clearly see that at approximately 0.1 ML (roughly 0.05 electron/Fe), a superconductinglike gap develops in all original nonsuperconducting films. The U-shaped gap with vanishing density of state at E_F is similar to that of 1-UC films on STO [1], primarily indicating nodeless pairing. With increasing K

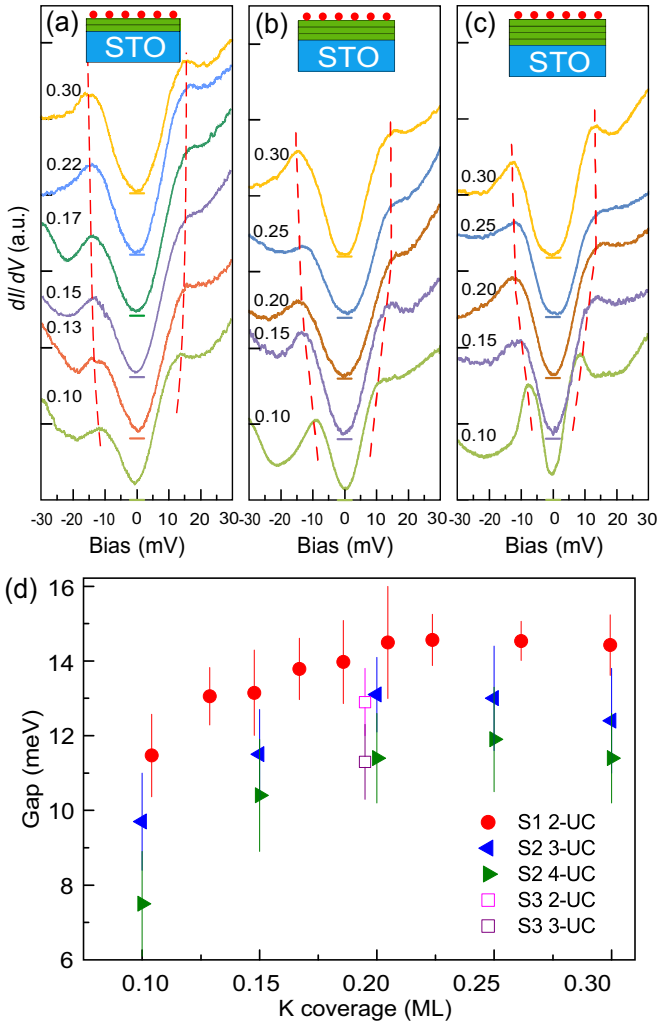

FIG. 2. Typical dI/dV curves taken on the 2-UC (a), 3-UC (b), and 4-UC (c) FeSe films at various K coverages ($V = 30$ mV, $I = 100$ pA). Each data point in the dI/dV spectra was obtained by averaging ten adjacent points. The horizontal bars indicate zero conductance position of each curve. The dashes are a guide for the eyes, showing the change of coherence peaks. (d) The dependence of the superconducting gaps on K coverage. Error bars are estimated from the standard deviation of Δ measured at various locations.

coverage, the magnitude of gap, defined by half the distance between the two sharp coherence peaks, increases and reaches a maximum value of 14.5 ± 1.0 meV, 13.1 ± 1.4 meV, and 11.9 ± 1.4 meV for 2-UC, 3-UC, and 4-UC films, respectively. The optimal K coverage, defined as the coverage at which the gap reaches maximum, for 2-4-UC films is found similar, 0.20-0.25 ML, which suggests that the charge transfer from K atoms occurs mainly in the topmost FeSe layer where K atoms are located. The optimal K coverage of 0.20–0.25 ML is coincident with the coverage at which significant cluster formation occurs. Further increasing K coverage alters the gap size little within experimental uncertainty. An intuitive explanation for this observation is clustering of K atoms, since clustering consumes electrons available for doping (Fig. S1). If assuming each individual K atom contributes one electron, this

consistent optimal K coverage of 0.20–0.25 ML approximately corresponds to a charge transfer concentration of 0.10–0.13 electron/Fe for all the K-coated 2–4-UC FeSe films (roughly equal to the value of 0.12 electron/Fe from STO to 1-UC FeSe films [3,4]). However, the maximum magnitude of superconducting gap systematically decreases with the doped layer being away from the FeSe/STO interface, explicitly indicating an additional interface enhance effect which is most probably e-ph coupling as evidenced below. It is worth noting that similar spectra within an energy range of $\pm$ 50 meV were obtained on K atoms and the exposed FeSe surface, except that the coherent peaks on K atoms are suppressed (Fig. S2). This result provides further support to the plain s-wave nature of the pairing as revealed by a recent STS study [29].

The second important finding of this study is the observation of characteristic bosonic modes. The data for bare 1-UC films and K-coated 3-UC films are shown in Figs. 3(a) and 3(b), respectively. We choose particularly these two cases for detailed discussion since their superconductivity has been demonstrated by ARPES [2–5,16] and transport experiments [7–10]. In addition to the superconducting gap $\Delta\sim$17.5 and $\sim$11.7 meV, we can see some satellite dip-hump features outside the coherence peaks [Figs. 3(a) and 3(b), top panels]. These features are more clearly identified in the normalized dI/dV spectrum [Figs. 3(a) and 3(b), middle panels], and bear a striking resemblance to those of phonons observed in Pb [18,19]. We temporally assign these dip-hump features to quasiparticle coupling to certain collective bosonic excitations. To read out the bosonic mode energy, we calculated numerically the second derivative of the tunneling conductance [Figs. 3(a) and 3(b), bottom panels]. By subtracting $\Delta\sim$17.5 (11.7) meV from the two dips (peaks) at energies of + (−) 28.2 (21.7) meV and + (−) 37.3 (34.0) meV, we obtained the energies of two bosonic modes for bare 1-UC FeSe films (K-coated 3-UC FeSe films) $\Omega_1 = 10.7$ (10.0) meV and $\Omega_2 = 19.8$ (22.3) meV, respectively.

The observation of the bosonic modes immediately raises a question whether and how they are linked to superconductivity. We then conducted an extensive variable temperature (4.6–30.2 K) STS experiment to identify its nature. The result for K-coated 2-UC films is shown in Fig. 3(c). With increasing temperature, the dip-hump features and the superconducting coherent peaks tend to degrade simultaneously and disappear eventually, suggesting that they are intertwined. For a more quantitative analysis, we measured the mode energy Ω from the STS spectra of superconducting films, including bare 1-UC films and K-coated 2-4-UC films at various K coverage (Fig. S3), and summarized the data in Fig. 3(d). Depending on the film thickness and K coverage, the superconducting gap changes significantly from 6.5 to 19 meV. The large fluctuation in superconducting gap for given thickness and K coverage is due probably to sample quality change in different runs of experiment, which is not a central problem of this study and will not be discussed here. Regardless of this variation, however, we see that the energy distribution of the bosonic modes collapses basically into two distinct groups, the first centered at 11.0 meV ($\Omega_1 = 11.0 \pm 2.1$ meV) and the second at 21.5 meV ($\Omega_2 = 21.5 \pm 4.5$ meV). This points out two characteristic energy scales for the bosonic modes in the system, which we emphasize are basically independent of

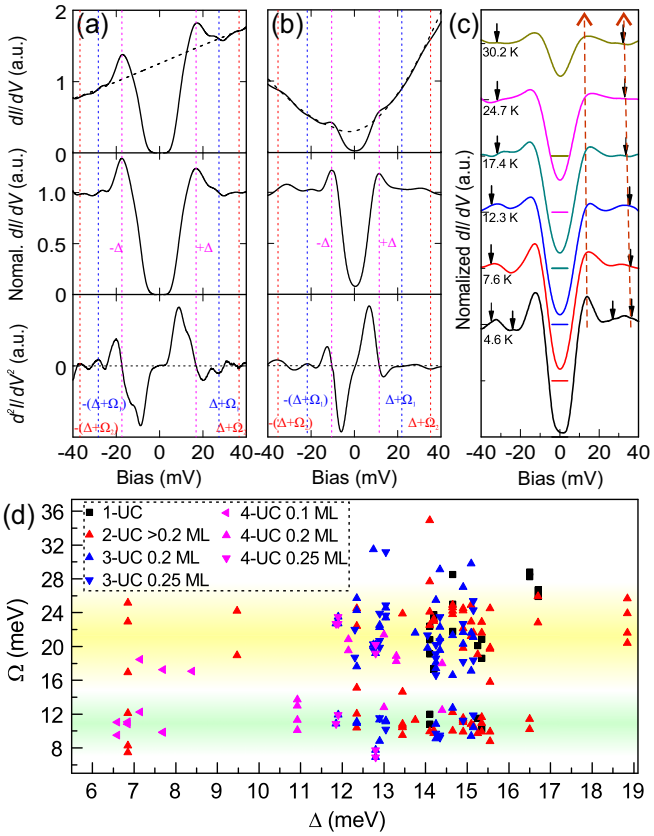

FIG. 3. (a) and (b) Black curves show raw dI/dV (top panel, $V = 50$ mV, $I = 100$ pA), normalized dI/dV (middle panel), and d^2I/dV^2 (bottom panel) spectra on bare 1-UC films and 3-UC films at the K coverage of 0.20 ML, respectively. The normalization was performed by dividing the raw dI/dV spectrum by its background, which was extracted from a cubic fit to the conductance for $|V| >$ 20 mV (the dashed line in the top panel). The pink, blue, and red dashes show the approximate energy positions of $\pm\Delta$, $\pm(\Delta + \Omega_1)$ and $\pm(\Delta + \Omega_2)$, respectively. (c) Normalized dI/dV spectra ($V = 50$ mV, $I = 100$ pA) at temperatures ranging from 4.6 to 30.2 K taken on 2-UC FeSe films at the K coverage of 0.20 ML. The horizontal bars indicate zero conductance position of each curve. The pink dashes and the red dashes are parallel and show the synchronous change in coherence peak and feature of phonon Ω_2. The spectra in (a)-(c) are smoothed by Gaussian filtering. (d) The distribution of the phonon energy Ω as a function of the superconducting gap magnitude Δ.

doping level (K coverage) and film thickness in the range of 1–4 UC.

We note that there is a striking consistency between the bosonic modes at $\Omega_1 = 11.0$ meV and $\Omega_2 = 21.5$ meV in the aforementioned superconducting films and the phonon frequencies in bulk materials. According to previous neutron scattering and Raman scattering measurements [30–32], the bulk FeSe exhibits E_g(Se) phonons at frequencies of 12–13.1 meV and A_{1g}(Se) phonons at frequency $\sim$19.8 meV, while STO has a TO_2 phonon with frequency of 21.7 meV. Albeit subtle change in frequency at surface/interface and probably further change caused by K adsorption, this agreement justifies our measurement and strongly suggests that the two bosonic

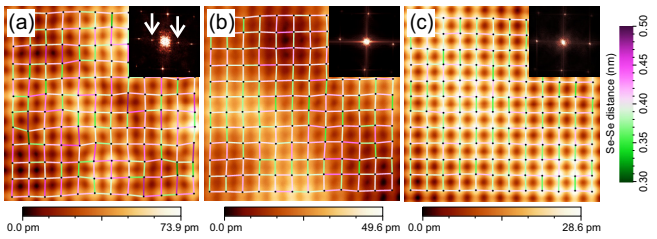

FIG. 4. Atomically resolved images ($V = 100$ mV, $I = 100$ pA, 4.8 nm $\times$ 4.8 nm) of 1-UC (a), 2-UC (b), and 3-UC FeSe (c) films acquired on one single sample. Local maxima (black dots) are used as approximate positions of the Se atoms; the distances between adjacent atoms are manifested by the colored segments. The insets fast Fourier transformation images based on an area of 30 nm $\times$ 30 nm showing a consistent lattice constant of $\sim$0.39 nm. The arrows in (a) label the spots corresponding to the 2 $\times$ 1 electronic structure, which is a unique feature of 1-UC films.

modes are phonons. Therefore, the features in tunneling spectra shown in Fig. 3 correspond to the quasiparticle coupling to the phonons at $\sim$11.0 and $\sim$21.5 meV and hence indicate that e-ph coupling plays a vital role in electron pairing in ultrathin FeSe films on STO. In sharp contrast, in ultrathin films of FeSe grown on and weakly bonded to graphene that we previously studied [12,33], the superconducting gap decreases with decreasing film thickness and is vanishing for 1-UC films. Although a bosonic mode was also observed, the energy is smaller and only in a level of 2.7-4 meV [25]. These differences point out a special role of the STO substrate in the high-T_C superconductivity in ultrathin films of FeSe we studied here.

The template effect in 1-UC FeSe films on STO was recently investigated theoretically [34]. According to the first-principles calculations, the STO substrate stabilizes the 1-UC FeSe films to a nearly square arrangement so as to prevent the films from undergoing a shear-type structure transition as the case in bulk. Indeed, the atomically resolved STM images of 1–3-UC FeSe films in Fig. 4 show that the films all exhibit a square lattice with a consistent in-plane lattice constant $\sim$0.39 nm (although local distortion becomes weaker with increasing thickness), indicative of significant template effect from the STO substrate. As a result, two e-ph coupling channels are opened and enhanced by the interface effect, which leads to an e-ph coupling constant $\lambda = 1.6$ which is ten times that ($\lambda = 0.16$) of bulk FeSe [35]. The phonon frequencies involved in the coupling discovered from the calculations are 10 and 20 meV [34], which are, again, in excellent agreement with $\Omega_1 \sim 11.0$ meV and $\Omega_2 \sim 21.5$ meV for 1-4-UC films observed experimentally here.

The interface promoted e-ph coupling is further supported by recent ARPES studies [5,36]. The study with femtosecond time resolution not only identifies a group of phonons with a frequency consistent with the phonon mode Ω_2, but also reveals that the phonons become soft at the interface [36]. The phonon softening at the interface has long been known as an effective way to enhance e-ph coupling strength and to raise T_C, as demonstrated in the early study of conventional superconductor multilayers [37]. Coupling to high-frequency phonons is necessary to account for the high T_C in the ultrathin FeSe films on STO [34]; indeed, oxygen optical phonons at 100 meV were disclosed experimentally [5]. Although quantitative agreement in T_C between the experiments and theories has not been reached at this stage, all available findings, such as the thickness dependence of the superconducting gap in K-coated ultrathin FeSe films on STO (Fig. 2), the evidence of e-ph coupling (Fig. 3 and Ref. [5]), the U-shaped gap [1,38], and so on, can qualitatively be understood consistently within the interface-enhanced e-ph coupling scenario.

The interface-enhanced e-ph coupling and hence high-T_C superconductivity is also revealed in 1-UC $FeTe_{1-x}Se_x$ films on STO. In this case, the U-shaped superconducting gaps range from 13 to $\sim$16.5 meV [39], nearly ten times the gap value ($\sim$1.7 meV) of the optimally doped bulk $FeTe_{0.6}Se_{0.4}$ single crystal [40]. Several groups of phonons with frequencies of $\sim$10, $\sim$20, and $\sim$25 meV are observed on 1-UC $FeTe_{1-x}Se_x$ films ($0.1 \leqslant x \leqslant 0.6$) on STO (Fig. S4). These phonon modes are consistent with E_g(Te/Se), A_{1g}(Te/Se)/TO_2(STO), and B_{1g}(Fe) modes, respectively, observed in previous Raman and neutron scattering studies [32,41,42]. The spin resonance mode at $\sim$6 meV [43,44] is not observed. The above result indicates that interface-enhanced e-ph coupling is a rather general approach for raising superconductivity temperature.

Finally, we briefly comment on the interpretation of the dome-shaped superconducting phase diagram in terms of interface-enhanced antiferromagnetic fluctuation [16]. Within the antiferromagnetic fluctuation scenario, different doping levels should alter spin fluctuation by promoting different ordered phases and change the spin resonance energy [24,45]. However, what we observed is that the mode energies are independent of the superconducting gap and doping level, as shown in Fig. 3(d). On the other hand, because of the change of screening [46], the amplitude of e-ph coupling can be doping dependent. And, quasiparticle scattering from K atoms/clusters can also lead to suppression of superconductivity (Fig. S2), and thus contribute to the dome-shaped superconducting phase diagram.

In summary, our study demonstrates that 2-4-UC FeSe films on STO exhibit thickness-dependent superconducting gaps larger than 11 meV under optimal surface doping of K atoms/clusters and interface-enhanced e-ph coupling is the most plausible mechanism for the high-temperature superconductivity in ultrathin FeSe films on STO. This finding strongly suggests that, in order to understand the high-T_C mechanism in cuprates, it is crucial to prepare the CuO_2 layer either by growth or by vacuum cleaving of the single crystal material and conduct direct measurement on the CuO_2 surface, which is currently underway in our group. Motivated by this work, we propose to fabricate a heterostructure where 2-3-UC FeSe is sandwiched between STO on both sides or STO on one side and $A_xFe_{2-y}Se_2$ (A = K, Rb, Cs, Tl/K) on the other side to achieve higher T_C.

This work is supported by NSFC (Grants No. 91421312 and No. 11574174) and MOST of China (Grant No. 2015CB921000).

C.J. Tang and C. Liu contributed equally to this work.

[1] Q.-Y. Wang, Z. Li, W.-H. Zhang, Z.-C. Zhang, J.-S. Zhang, W. Li, H. Ding, Y.-B. Ou, P. Deng, K. Chang, J. Wen, C.-L. Song, K. He, J.-F. Jia, S.-H. Ji, Y.-Y. Wang, L.-L. Wang, X. Chen, X.-C. Ma, and Q.-K. Xue, Chin. Phys. Lett. **29**, 037402 (2012).

[2] D. F. Liu, W. H. Zhang, D. X. Mou, J. F. He, Y. B. Ou, Q. Y. Wang, Z. Li, L.-L. Wang, L. Zhao, S. L. He, Y. Y. Peng, X. Liu, C. Y. Chen, L. Yu, G. D. Liu, X. L. Dong, J. Zhang, C. T. Chen, Z. Y. Xu, J. P. Hu, X. Chen, X. C. Ma, Q.-K. Xue, and X. J. Zhou, Nat. Commun. **3**, 931 (2012).

[3] S. L. He, J. F. He, W. H. Zhang, L. Zhao, D. F. Liu, X. Liu, D. X. Mou, Y. B. Ou, Q. Y. Wang, Z. Li, L.-L. Wang, Y. Y. Peng, Y. Liu, C. Y. Chen, L. Yu, G. D. Liu, X. L. Dong, J. Zhang, C. T. Chen, Z. Y. Xu, X. Chen, X. C. Ma, Q.-K. Xue, and X. J. Zhou, Nat. Mater. **12**, 605 (2013).

[4] S. Y. Tan, Y. Zhang, M. Xia, Z. R. Ye, F. Chen, X. Xie, R. Peng, D. F. Xu, Q. Fan, H. C. Xu, J. Jiang, T. Zhang, X. C. Lai, T. Xiang, J. P. Hu, B. P. Xie, and D. L. Feng, Nat. Mater. **12**, 634 (2013).

[5] J. J. Lee, F. T. Schmitt, R. G. Moore, S. Johnston, Y. T. Cui, W. Li, M. Yi, Z. K. Liu, M. Hashimoto, Y. Zhang, D. H. Lu, T. P. Devereaux, D. H. Lee, and Z. X. Shen, Nature (London) **515**, 245 (2014).

[6] X. Liu, D. F. Liu, W. H. Zhang, J. F. He, L. Zhao, S. L. He, D. X. Mou, F. S. Li, C. J. Tang, Z. Li, L.-L. Wang, Y. Y. Peng, Y. Liu, C. Y. Chen, L. Yu, G. D. Liu, X. L. Dong, J. Zhang, C. T. Chen, Z. Y. Xu, X. Chen, X. C. Ma, Q.-K. Xue, and X. J. Zhou, Nat. Commun. **5**, 5047 (2014).

[7] W.-H. Zhang, Y. Sun, J.-S. Zhang, F.-S. Li, M.-H. Guo, Y.-F. Zhao, H.-M. Zhang, J.-P. Peng, Y. Xing, H.-C. Wang, T. Fujita, A. Hirata, Z. Li, H. Ding, C.-J. Tang, M. Wang, Q.-Y. Wang, K. He, S.-H. Ji, X. Chen, J.-F. Wang, Z.-C. Xia, L. Li, Y.-Y. Wang, J. Wang, L.-L. Wang, M.-W. Chen, Q.-K. Xue, and X.-C. Ma, Chin. Phys. Lett. **31**, 017401 (2014).

[8] L. Z. Deng, B. Lv, Z. Wu, Y. Y. Xue, W. H. Zhang, F. S. Li, L.-L. Wang, X. C. Ma, Q.-K. Xue, and C. W. Chu, Phys. Rev. B **90**, 214513 (2014).

[9] J. F. Ge, Z. L. Liu, C. Liu, C. L. Gao, D. Qian, Q.-K. Xue, Y. Liu, and J. F. Jia, Nat. Mater. **14**, 285 (2015).

[10] Z. C. Zhang, Y.-H. Wang, Q. Song, C. Liu, R. Peng, K. A. Moler, D.-L. Feng, and Y.-Y. Wang, Sci. Bull. **60**, 1301 (2015).

[11] F. C. Hsu, J. Y. Luo, K. W. Yeh, T. K. Chen, T. W. Huang, P. M. Wu, Y. C. Lee, Y. L. Huang, Y. Y. Chu, D. C. Yan, and M. K. Wu, Proc. Natl. Acad. Sci. USA **105**, 14262 (2008).

[12] C.-L. Song, Y.-L. Wang, Y.-P. Jiang, Z. Li, L.-L. Wang, K. He, X. Chen, X.-C. Ma, and Q.-K. Xue, Phys. Rev. B **84**, 020503 (2011).

[13] J. Bang, Z. Li, Y. Y. Sun, A. Samanta, Y. Y. Zhang, W. Zhang, L.-L. Wang, X. Chen, X.-C. Ma, Q.-K. Xue, and S. B. Zhang, Phys. Rev. B **87**, 220503 (2013).

[14] P. A. Lee, N. Nagaosa, and X.-G. Wen, Rev. Mod. Phys. **78**, 17 (2006).

[15] G. R. Stewart, Rev. Mod. Phys. **83**, 1589 (2011).

[16] Y. Miyata, K. Nakayama, K. Sugawara, T. Sato, and T. Takahashi, Nat. Mater. **14**, 775 (2015).

[17] G. M. Eliashberg, Sov. Phys. JETP **11**, 696 (1960).

[18] J. M. Rowell, P. W. Anderson, and D. E. Thomas, Phys. Rev. Lett. **10**, 334 (1963).

[19] W. L. McMillan and J. M. Rowell, Phys. Rev. Lett. **14**, 108 (1965).

[20] D. J. Scalapino, J. R. Schrieffer, and J. W. Wilkins, Phys. Rev. **148**, 263 (1966).

[21] V. Z. Kresin and S. A. Wolf, Rev. Mod. Phys. **81**, 481 (2009).

[22] J. Lee, K. Fujita, K. McElroy, J. A. Slezak, M. Wang, Y. Aiura, H. Bando, M. Ishikado, T. Masui, J. X. Zhu, A. V. Balatsky, H. Eisaki, S. Uchida, and J. C. Davis, Nature (London) **442**, 546 (2006).

[23] H. Shim, P. Chaudhari, G. Logvenov, and I. Bozovic, Phys. Rev. Lett. **101**, 247004 (2008).

[24] L. Shan, J. Gong, Y.-L. Wang, B. Shen, X. Hou, C. Ren, C. Li, H. Yang, H.-H. Wen, S. Li, and P. Dai, Phys. Rev. Lett. **108**, 227002 (2012).

[25] C.-L. Song, Y.-L. Wang, Y.-P. Jiang, Z. Li, L.-L. Wang, K. He, X. Chen, J. E. Hoffman, X.-C. Ma, and Q.-K. Xue, Phys. Rev. Lett. **112**, 057002 (2014).

[26] C.-J. Tang, D. Zhang, Y.-Y. Zang, C. Liu, G.-Y. Zhou, Z. Li, C. Zheng, X.-P. Hu, C.-L. Song, S.-H. Ji, K. He, X. Chen, L.-L. Wang, X.-C. Ma, and Q.-K. Xue, Phys. Rev. B **92**, 180507(R) (2015).

[27] J.-G. Guo, S.-F. Jin, G. Wang, S.-C. Wang, K.-X. Zhu, T.-T. Zhou, M. He, and X.-L. Chen, Phys. Rev. B **82**, 180520 (2010).

[28] See Supplementary Material at http://link.aps.org/supplemental/10.1103/PhysRevB.93.020507 for description of tunneling spectra measurement and more *dI*/*dV* spectra.

[29] Q. Fan, W. H. Zhang, X. Liu, Y. J. Yan, M. Q. Ren, R. Peng, H. C. Xu, B. P. Xie, J. P. Hu, T. Zhang, and D. L. Feng, Nat. Phys. **11**, 946 (2015).

[30] D. Phelan, J. N. Millican, E. L. Thomas, J. B. Leão, Y. Qiu, and R. Paul, Phys. Rev. B **79**, 014519 (2009).

[31] P. Kumar, A. Kumar, S. Saha, D. V. S. Muthu, J. Prakash, S. Patnaik, U. V. Waghmare, A. K. Ganguli, and A. K. Sood, Solid State Commun. **150**, 557 (2010).

[32] N. Choudhury, E. J. Walter, A. I. Kolesnikov, and C.-K. Loong, Phys. Rev. B **77**, 134111 (2008).

[33] C.-L. Song, Y.-L. Wang, P. Cheng, Y.-P. Jiang, W. Li, T. Zhang, Z. Li, K. He, L.-L. Wang, J.-F. Jia, H. H. Hung, C. J. Wu, X.-C. Ma, X. Chen, and Q.-K. Xue, Science **332**, 1410 (2011).

[34] S. Coh, M. L. Cohen, and S. G. Louie, New J. Phys. **17**, 073027 (2015).

[35] C. W. Luo, I. H. Wu, P. C. Cheng, J. Y. Lin, K. H. Wu, T. M. Uen, J. Y. Juang, T. Kobayashi, D. A. Chareev, O. S. Volkova, and A. N. Vasiliev, Phys. Rev. Lett. **108**, 257006 (2012).

[36] S. Yang, J. A. Sobota, D. Leuenberger, A. F. Kemper, J. J. Lee, F. T. Schmitt, W. Li, R. G. Moore, P. S. Kirchmann, and Z. X. Shen, Nano Lett. **15**, 4150 (2015).

[37] M. Strongin, O. F. Kammerer, J. E. Crow, R.O.Parks, R.O.Parks, and M. A. Jesen, Phys. Rev. Lett. **21**, 1320 (1968).

[38] Z. Li, J. P. Peng, H. M. Zhang, W. H. Zhang, H. Ding, P. Deng, K. Chang, C. L. Song, S. H. Ji, L.-L. Wang, K. He, X. Chen, Q. K. Xue, and X. C. Ma, J. Phys.: Condens. Matter **26**, 265002 (2014).

[39] F.-S. Li, H. Ding, C.-J. Tang, J.-P. Peng, Q.-H. Zhang, W.-H. Zhang, G.-Y. Zhou, D. Zhang, C.-L. Song, K. He, S.-H. Ji, X. Chen, L. Gu, L.-L. Wang, X.-C. Ma, and Q.-K. Xue, Phys. Rev. B **91**, 220503 (2015).

[40] T. Hanaguri, S. Niitaka, K. Kuroki, and H. Takagi, Science **328**, 474 (2010).

[41] T. L. Xia, D. Hou, S. C. Zhao, A. M. Zhang, G. F. Chen, J. L. Luo, N. L. Wang, J. H. Wei, Z. Y. Lu, and Q. M. Zhang, Phys. Rev. B **79**, 140510 (2009).

[42] K. Okazaki, S. Sugai, S. Niitaka, and H. Takagi, Phys. Rev. B **83**, 035103 (2011).

[43] J.-S. Wen, G.-Y. Xu, Z.-J. Xu, Z. W. Lin, Q. Li, Y. Chen, S.-X. Chi, G.-D. Gu, and J. M. Tranquada, Phys. Rev. B **81**, 100513 (2010).

[44] Y.-M. Qiu, W. Bao, Y. Zhao, C. Broholm, V. Stanev, Z. Tesanovic, Y. C. Gasparovic, S. Chang, J. Hu, B. Qian, M.-H. Fang, and Z.-Q. Mao, Phys. Rev. Lett. **103**, 067008 (2009).

[45] H. He, Y. Sidis, P. Bourges, G. D. Gu, A. Ivanov, N. Koshizuka, B. Liang, C. T. Lin, L. P. Regnault, E. Schoenherr, and B. Keimer, Phys. Rev. Lett. **86**, 1610 (2001).

[46] W. Meevasana, N. J. C. Ingle, D. H. Lu, J. R. Shi, F. Baumberger, K. M. Shen, W. S. Lee, T. Cuk, H. Eisaki, T. P. Devereaux, N. Nagaosa, J. Zaanen, and Z. X. Shen, Phys. Rev. Lett. **96**, 157003 (2006).